Three-Dimensional Topographic Angiography in Chorioretinal Vascular Disease

Ursula Schmidt-Erfurth,[1] *Sven Teschner,*[1] *Joachim Noack,*[2] *and Reginald Birngruber*[2]

Purpose. To evaluate a new angiographic technique that offers three-dimensional imaging of chorioretinal vascular diseases.

Methods. Fluorescein (FA) and indocyanine green angiography (ICGA) were performed using a confocal scanning laser ophthalmoscope. Tomographic series with 32 images per set were taken over a depth of 4 mm at an image frequency of 20 Hz. An axial analysis was performed for each *x/y* position to determine the fluorescence distribution along the *z*-axis. The location of the onset of fluorescence at a defined threshold intensity was identified and a depth profile was generated. The overall results of fluorescence topography were displayed in a gray scale–coded image and three-dimensional relief.

Results. Topographic angiography delineated the choriocapillary surface covering the posterior pole with exposed larger retinal vessels. Superficial masking of fluorescence by hemorrhage or absorbing fluid did not preclude detection of underlying diseases. Choroidal neovascularization (CNV) appeared as a vascular formation with distinct configuration and prominence. Chorioretinal infiltrates exhibited perfusion defects with dye pooling. Retinal pigment epithelium detachments (PEDs) demonstrated dynamic filling mechanisms. Intraretinal extravasation in retinal vascular disease was detected within a well-demarcated area with prominent retinal thickening.

Conclusions. Confocal topographic angiography allows high-resolution three-dimensional imaging of chorioretinal vascular and exudative diseases. Structural vascular changes (e.g., proliferation) are detected in respect to location and size. Dynamic processes (e.g., perfusion defects, extravasation, and barrier dysfunction) are clearly identified and may be quantified. Topographic angiography is a promising technique in the diagnosis, therapeutic evaluation, and pathophysiological evaluation of macular disease. (*Invest Ophthalmol Vis Sci.* 2001;42:2386–2394)

Chorioretinal vascular disease of the macular area (e.g., diabetic maculopathy [DMP] and age-related macular degeneration [ARMD]) are the main reasons for progressive and severe visual loss by occlusive, proliferative, and/or exudative mechanisms.[1,2] Fluorescein angiography (FA) is the classic diagnostic tool but is often compromised by masking phenomena as a consequence of the short wavelength used. Diffuse leakage of the small fluorescein molecule causes further difficulties in identifying the origin and quantifying the dynamics of leakage. Despite stereoscopic viewing systems, many lesions remain occult, and prominence and extent of exudation are evaluated only subjectively.[2,3]

Indocyanine green angiography (ICGA) is effective in the near-infrared spectrum which allows improved transmission, and, mostly bound to albumin, it is thought to extravasate minimally.[4] ICGA should therefore improve imaging of occult lesions and identification of origins of leaking diseases.[5–7] Scanning laser ophthalmoscopy (SLO), with point-source illumination and optimized excitation, has further enhanced diagnostic efficacy.[8] The confocal SLO mode combines optimal contrast, high sensitivity, and depth resolution.[9,10] The option to scan through different retinal layers is nevertheless limited to a depth resolution of approximately 300 μm. It may be used, however, to obtain topographic profiles of strongly reflecting intraocular structures, such as the optic disc and the macular region.[11]

Morphometric imaging of vascular structures of retina and choroid would significantly improve the diagnosis of macular disease. A novel angiographic technology, confocal topographic angiography, has been developed that allows three-dimensional (3-D) documentation of vascular structures and characterization of dynamic phenomena such as perfusion and leakage. The technique of topographic image processing was applied in the FA and ICGA analyses of representative types of chorioretinal vascular disease, to document structural and dynamic changes and to evaluate the diagnostic potential of the new method.

Materials and Methods

The basic topographic principle is to use a series of lateral confocal optical sections of the chorioretinal fluorescence distribution and, by introducing a smart algorithm, to extract the 3-D profile of the surface of vascular structures and related leakage. Data acquisition was achieved with a conventional confocal scanning laser angiograph. Data processing and topographic analysis were performed on a standard desktop computer, using newly developed software. The method of confocal laser scanning topography based on ICGA has been published.[12,13]

Data Acquisition

FA and ICGA were performed using a confocal SLO (Heidelberg Retina Angiograph; Heidelberg Engineering, Dossenheim, Germany). Infrared images were taken for optical alignment with the fovea in the center of a 30° field corresponding to a retinal area of 9 × 9 mm. For FA, 5 ml of 10% fluorescein solution (Alcon Pharma GmbH, Freiburg, Germany), an argon laser emitting at 488 nm for excitation, and filters blocking transmission of wavelengths below 510 nm were used for detection. For ICGA a 50-mg solution of ICG (ICG Pulsion, München, Germany) was administered intravenously, and excitation and detection were performed, using a diode laser emitting at 795 nm and blocking filters for wavelengths below 835 nm. The diameter of the excitation beam was 10 μm at the retina. The Rayleigh range of the focal beam's waist determining depth resolution was 300 μm. During the early transit phase, the scanning laser was focused onto the retinal vessels and the excitation intensity was adjusted to obtain adequate illumination. An additive +3-diopter (D) refractive correction was added by using the internal focus adjustment to create a preretinal initial focus for complete sectioning of elevated lesions. An early FA/ICGA series of 32 tomographic sections was taken over a depth of 4 mm, each separated

From the [1]University Eye Hospital, Lübeck, Germany; and the [2]Medical Laser Center, Lübeck, Germany.

Submitted for publication February 12, 2001; revised April 30, 2001; accepted May 15, 2001.

Commercial relationships policy: N.

The publication costs of this article were defrayed in part by page charge payment. This article must therefore be marked "*advertisement*" in accordance with 18 U.S.C. §1734 solely to indicate this fact.

Corresponding author: Ursula Schmidt-Erfurth, University Eye Hospital, Ratzeburger Allee 160, D-23538, Lübeck, Germany.
uschmidterfurth@ophtha.mu-luebeck.de

Investigative Ophthalmology & Visual Science, September 2001, Vol. 42, No. 10

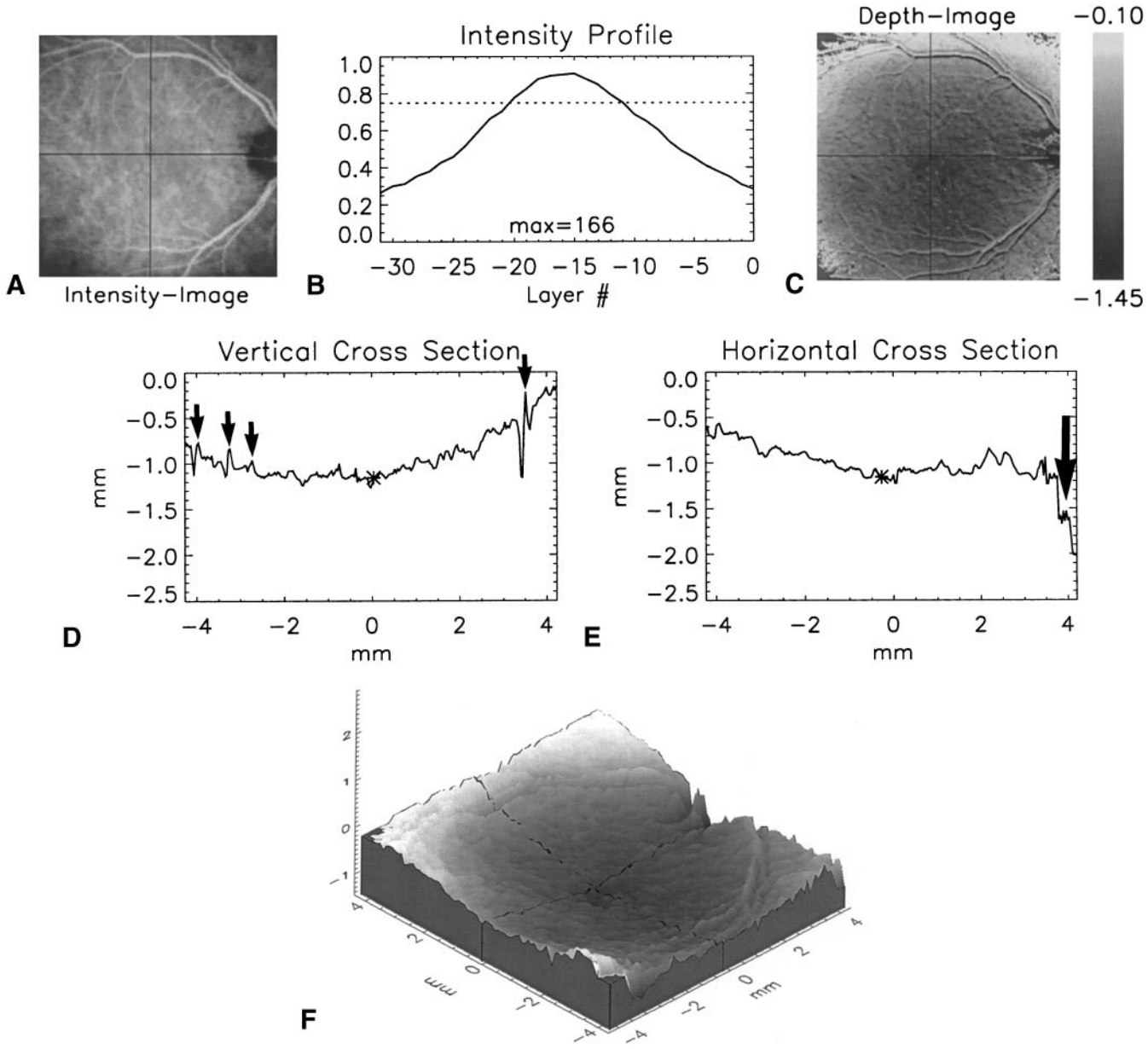

FIGURE 1. (**A**) The ICG intensity profile indicates areas with high or low absolute fluorescence levels; bright, high intensity; dark, low intensity. (**B**) The distribution of choroidal ICG fluorescence along the *z*-axis is documented at a given *x/y* position. (**C**) The gray scale–coded 2-D depth profile demonstrates the distribution of axial fluorescence within the entire angiographic field; bright, prominent localization; dark, deep localization. (**D**) The vertical cross section delineates the surface of the intensity threshold along a 12- to 6-o'clock axis through the macula (*asterisk*) and indicates the location of prominent retinal vessels (*arrows*). (**E**) Horizontal cross section delineates the surface fluorescence along a 9- to 3-o'clock axis through the macula (*asterisk*) and optic nerve (*arrow*). (**F**) Three-dimensional relief displays the axial fluorescence topography within the entire field.

by 125 μm. A late series was produced after 10 minutes during FA and after 15 minutes during ICGA. Each data set was recorded within 1.6 seconds and was digitized to a grid of 256 × 256 pixels with an 8-bit intensity resolution.

Data Processing

Recording image distortions originating from the resonant line scanner were corrected. All images from a tomographic series were aligned to correct for artifacts caused by eye movements. Rotational mismatch was usually small. Only translational movements were corrected based on the cross-correlation calculated in the Fourier domain. To reduce the impact of local image distortions remaining after the alignment, a lateral averaging over a 3 × 3-pixel area was performed within each series. Subsequently, an intensity image was generated based on the maximum fluorescence intensity for each image point of the 32 aligned sections. The resultant intensity image indicated areas with high (bright) or low (dark) amounts of fluorescent marker and was consistent with a contrast-enhanced version of conventional FA or ICGA (Fig. 1A).

Topographic Analysis

To determine the depth distribution of fluorescence within the individual serial planes, the axial intensity profile was extracted from the aligned stack of cross-sectional images for each point in the *x/y* plane. The location of the onset of fluorescence at a defined threshold intensity was identified and a depth profile was generated. In an area with

Table 1. Disease Entities in Subgroups Undergoing Topographic Angiography, with Pathologic Correlate Identified

Disease	Eyes (*n*)	Procedure	Pathologic Correlate (*n*)
Normal condition	5	FA/ICGA	No pathology (5)
Hemorrhagic CNV	6	ICGA	Prominence (6)
Occult CNV component	16	ICGA	Prominence (16)
Chorioretinal infiltrates	5	ICGA	Defect/pooling (5)
Serous PED	8	FA/ICGA	Exudation (8)
Branch retinal vein occlusion	8	FA	Retinal extravasation (8)

physiological chorioretinal vasculature, the topographic intensity distribution in the *z*-axis resembled a bell-shaped curve (Fig. 1B). The curve had its maximum at the level of the choriocapillaris or the large retinal vessels with the highest dye concentration at physiological conditions. The depth value on the *z*-axis indicated the precise location of threshold fluorescence for each lateral position. This site are always situated on the surface of the fluorescent structure whether it be physiological (e.g., retinal vasculature) or pathologic (e.g., prominent choroidal neovascularization or leakage). The depth location was independent of the absolute intensity of fluorescence and depended only on the axial position where fluorescence appeared first.

Image Presentation

A two-dimensional (2-D) depth profile was obtained indicating the axial position of the onset of fluorescence plotted as a gray-scale image using a code of 256 scales (Fig. 1C). Superficial localization appeared bright, and fluorescence from deeper layers appeared dark. Horizontal and vertical cross sections (Figs. 1D, 1E) represented the topographic profile of the fluorescent surface at a given position. Areas with prominence or depression could be imaged selectively and differences in height could be measured quantitatively in micrometers. A qualitative representation was provided by imaging the topographic data set in a 3-D relief (Fig. 1F). Areas with very weak fluorescence or areas where the highest tomographic section of the series already exceeded the threshold criterion did not allow a reliable determination of fluorescence onset. Signals had to be above background threshold—that is, the difference of the maximal intensity and the minimal intensity of each axial scan had to be at least a factor of 2 and at least 75% of all data points had to be located within the 32 sections taken. The selection of this threshold was extremely critical. We preferred to lose some data points rather than adopt data that might be artifactual. These regions are shown as blank areas to avoid incorrect assumptions. The numbers on the gray scale alongside every topographic fluorescence image indicate the prominence of the lesion in millimeters.

Patient Selection

Forty-eight patients were examined by topographic angiography. Informed consent was obtained from all patients before any angiographic procedure was performed in compliance with the tenets of the Declaration of Helsinki. Five eyes had no clinical signs of disease, and 43 eyes showed macular degeneration with a chorioretinal vascular pathology. To evaluate diagnostic efficacy, topographic angiography was performed in five different entities: a normal chorioretinal condition ($n = 5$), CNV ($n = 22$), inflammatory choroidal disease ($n = 5$), RPE barrier dysfunction ($n = 8$), and retinal extravasation ($n = 8$). Patients with a neovascular disease were selected for detection of a potential vascular prominence by topographic ICGA in cases with failure of conventional ICGA to detect a vascular structure (e.g., hemorrhagic CNV and occult components of CNV). Chorioretinal infiltrates underwent topographic ICGA in an effort to detect a localized choroidal alteration. In serous pigment epithelial detachment (PED) the mechanism of isolated leakage was studied using topographic FA and ICGA. In branch retinal vein occlusion (BRVO), extravasation from retinal vessels was monitored by topographic FA. The specific subgroups are summarized in Table 1.

Results

Physiologic Condition

Topographic angiography generates a characteristic image of the vasculature of the posterior pole that differs substantially from conventional FA and ICGA. ICGA was selected to present choroidal structures with more detail than in FA, but both entities produce basically identical features. The classic ICG intensity image of a normal fundus was defined by the bright fluorescence of the retinal arcades and the homogenous background texture of the choroidal network (Fig. 1A). Extraction of the axial fluorescence distribution identified the prominence of the retinal vessels, whereas the relative depth of the

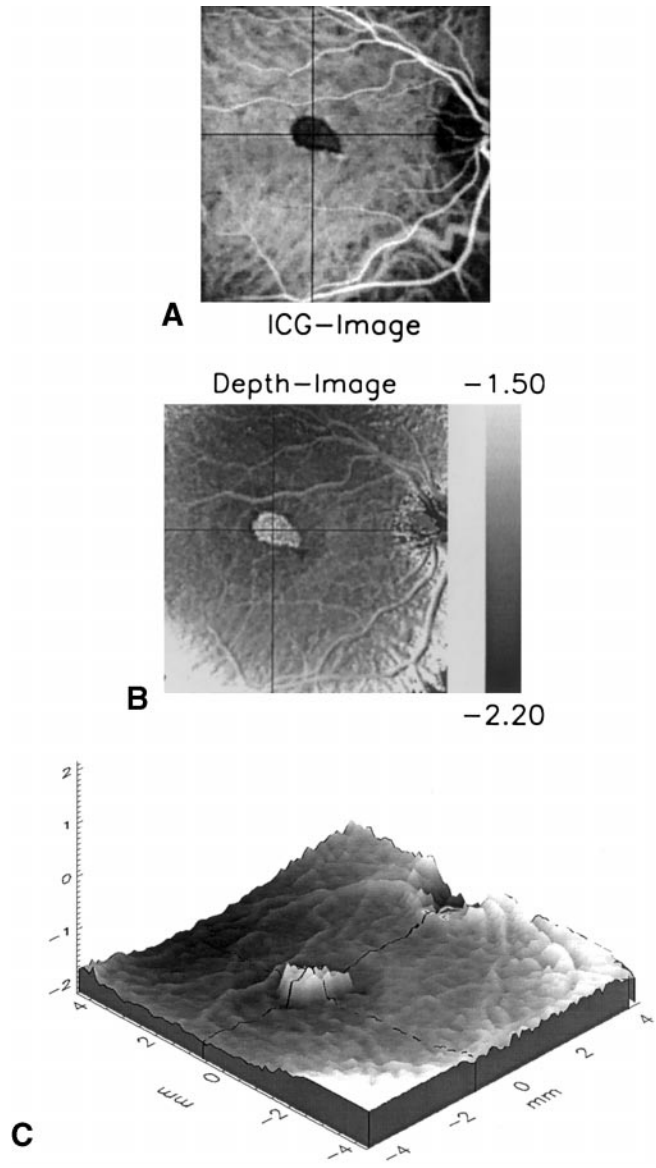

Figure 2. (**A**) Subretinal hemorrhage inhibits the detection of CNV by conventional ICGA. (**B**) Appearance of a bright signal in the gray-scale–coded depth profile indicates the presence of prominent fluorescence. (**C**) An elevated neovascular complex is surrounded by an area with depression of the choriocapillary surface.

macular choroidal surface was reflected by a central reduction in brightness (Fig. 1C). The cross sections delineated the choriocapillary layer with the prominent signals of the retinal vessels in the vertical section (Fig. 1D) and the depression of the optic nerve head in the horizontal section (Fig. 1E). The 3-D display offered a complete view of the vascular anatomy with the choroidal surface, the overlying retinal vessels, and the excavation of the optic nerve head (Fig. 1F).

CNV with Hemorrhage

CNV served as an example of proliferative disease. When hemorrhage was present, imaging was inhibited by masking in FA, and even ICGA may have failed to detect the underlying neovascular lesion (Fig. 2A). Axial analysis was able to detect fluorescence underlying a superficial layer of blood and depicted a distinct neovascular net (Fig. 2B). The 3-D display remodeled the exact site, height, and configuration of the prominent neovascular complex (Fig. 2C). In an additional finding, a dark halo seen in the depth profile (Fig. 2B) may indicate a loss in choroidal thickness (Fig. 2C). Neovascular prominence was seen in all eyes in this group.

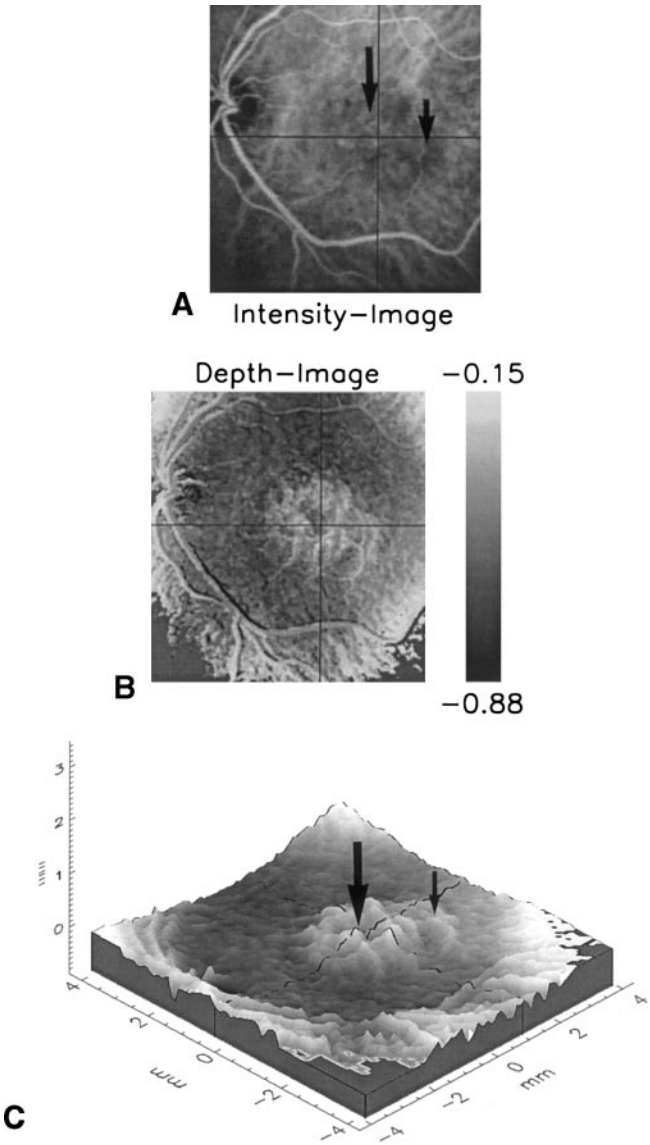

FIGURE 3. (**A**) ICGA images CNV with combined classic (*long arrow*) and occult (*short arrow*) components. (**B**) The demarcation of the neovascular complex is enhanced by the depth analysis. (**C**) By 3-D topography the classic component is seen as central island (*large arrow*), the occult portion imposes temporally as additional elevation (*small arrow*).

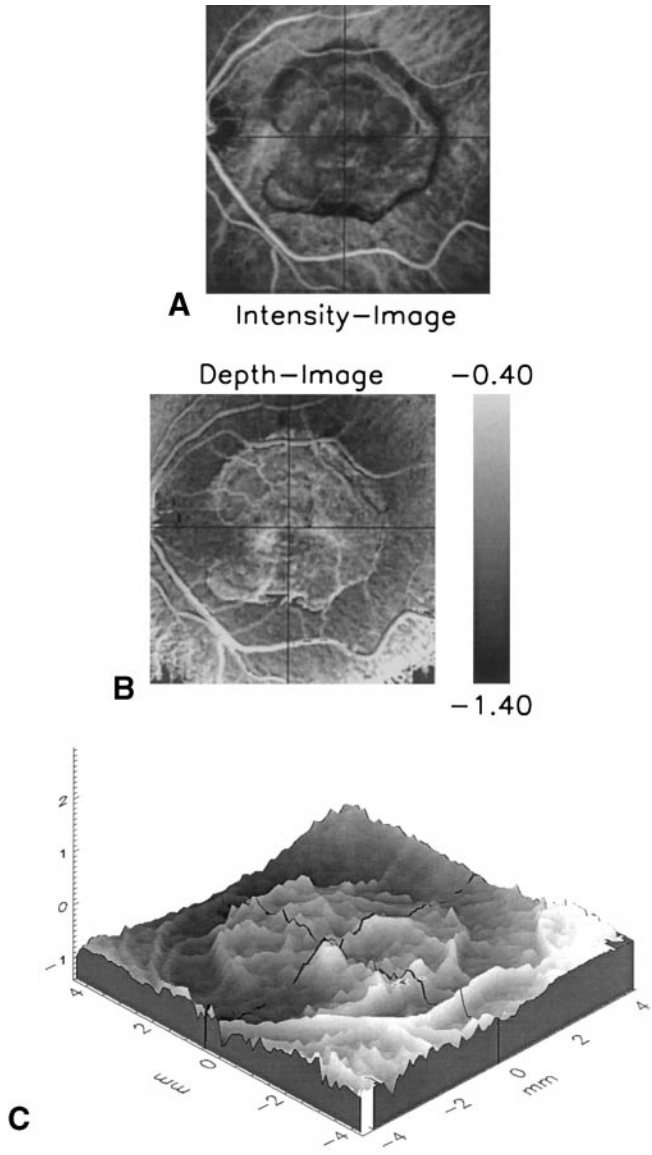

FIGURE 4. (**A**) Conventional ICGA of the CNV shown in Figure 3 exhibits progressive scarring 3 months later. (**B**) Depth analysis detects active neovascularization in the central part and at the hypofluorescent margins. (**C**) By 3-D angiography the entire extent of the neovascular membrane is precisely delineated.

Occult CNV

Independent of masking, the entire extent of CNV was rarely detectable by conventional FA. In Figure 3 routine FA revealed a small classic component in the nasal portion of the macula only, whereas conventional ICGA demonstrated a larger CNV complex, with a mixed picture of neovascular and hypofluorescent areas temporally (Fig. 3A). Topographic ICGA clearly identified the vascular component with well-defined borders (Fig. 3B). An indentation in the center indicated less dense vascularization than in the periphery. The 3-D representation remodeled the volume and configuration of the entire com-

plex. A nasal portion with a central crater formation characteristic of a classic component was found surrounded by an elevated border of active proliferation.[13] The occult hypofluorescent component seen temporally in conventional ICGA was now imaged as a sickle-shaped, prominent satellite on the right margin (Fig. 3C).

Quantification of Progression

The potential for precise determination of lesion size became obvious when documenting progression. The CNV lesion presented in Figure 3 was re-examined 3 months later. Although fibrosis and vascular reorganization obscured the margins as well as the central structure of the CNV in conventional ICGA (Fig. 4A), the features of the lesion were better captured in the depth profile (Fig. 4B). Neovascular structures were also seen beyond the upper retinal arcade. Two centers with more intensive activity and prominent neovascular sprouts were present in the center (Fig. 4C). The section of the retinal vessels overlying the CNV prominence in the superior portion appeared brighter, which indicates a localized elevation.

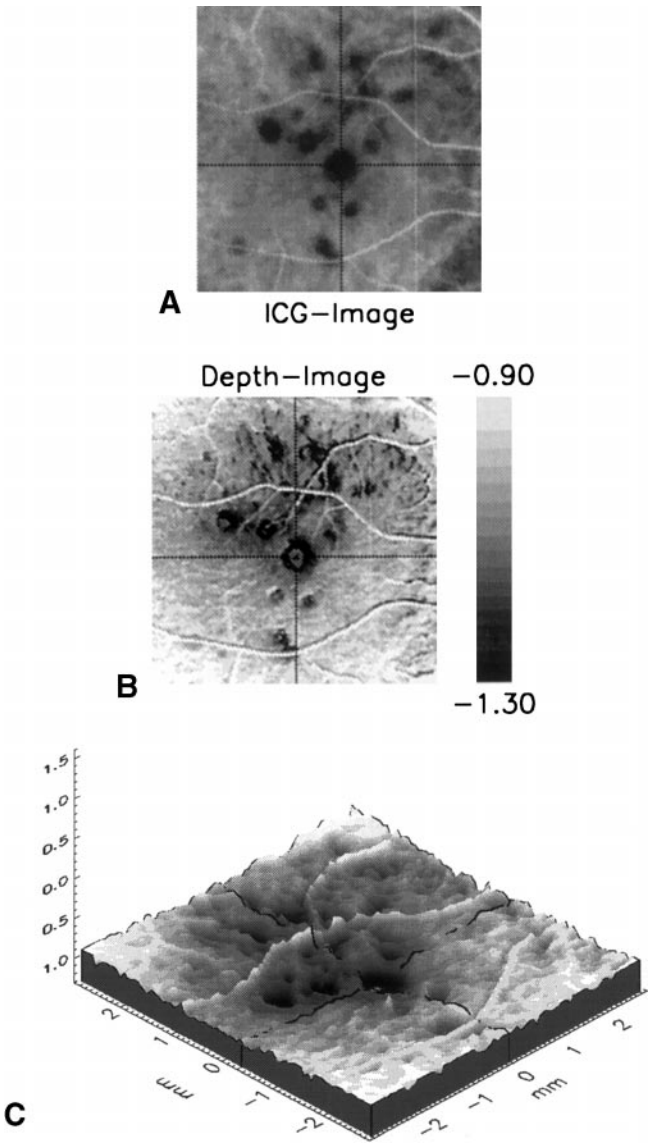

Figure 5. (**A**) Chorioretinal infiltrates are seen as blocked fluorescence by early-phase ICGA. (**B**) The gray-scaled depth image documents absence of fluorescence signals within the dark areas. (**C**) Topographic imaging reveals multiple perfusion defects within the choriocapillary layer.

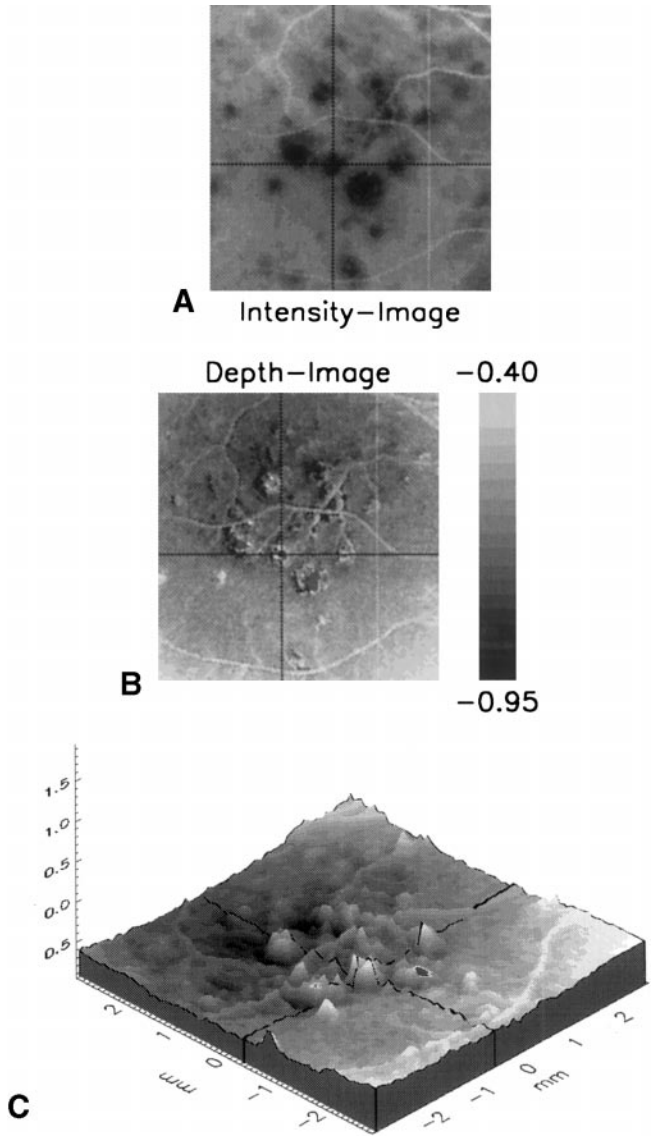

Figure 6. (**A**) Chorioretinal infiltrates appear unchanged during late-phase ICGA even at higher magnification. (**B**) Topographic analysis of late-phase fluorescence exhibits accumulation of dye within the dark lesions. (**C**) Active leakage is filling the choroidal perfusion defects with ICG seen as elevated peaks.

Inflammatory Chorioretinal Disease

Non-neovascular disease was mostly characterized by masking in conventional angiography, such as the localized infiltrates in chorioretinitis found by ICGA (Fig. 5A). Topographic ICGA during the early-phase confirmed hypofluorescence seen previously (Fig. 5A) with reduced or no fluorescence signals from superficial choroidal layers (Fig. 5B). Morphologically, the hypofluorescent areas corresponded to distinct filling defects within the choriocapillary layer (Fig. 5C). Late-phase conventional ICGA did not reveal any change in the appearance of the hypofluorescent spots over time (Fig. 6A). However, the depth profile had changed completely, with dark areas almost uniformly showing filling with ICG (Fig. 6B). By topography, the previously empty spaces were actively filling with fluid, indicating the exudative dynamics and the composition of the infiltrates of extravasate (Fig. 6C).

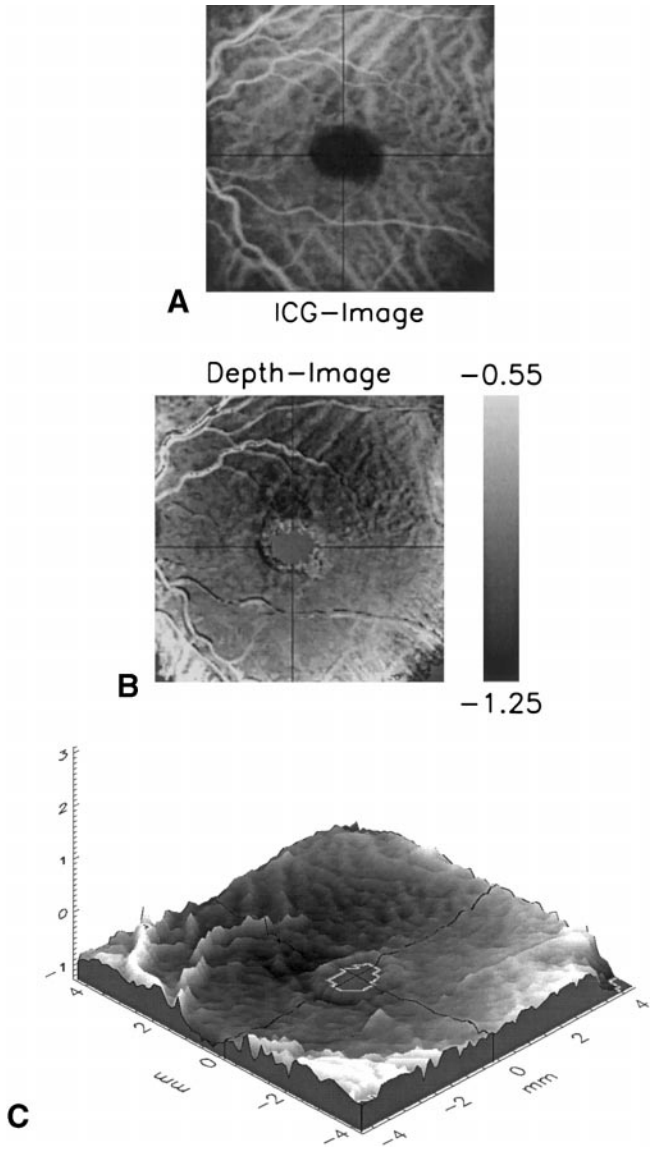

FIGURE 7. (**A**) Early-phase conventional ICGA shows hypofluorescence characteristic for PED. (**B**) In contrast to (**A**), fluorescence is present in a significant portion of the hypofluorescent area. (**C**) ICG is present at the basal portion of the PED in a flat distribution.

Pigment Epithelial Detachment

PED is referred to as the consequence of a localized exudation and/or failure of the RPE pump. Early conventional ICGA was unrevealing, because homogenous hypofluorescence covered the entire lesion site (Fig. 7A). Topographically relevant fluorescence was detected at least in the peripheral portion (Fig. 7B), consistent with the presence of ICG at the bottom of the PED or beginning exudation (Fig. 7C). Two-dimensional ICGA at 15 minutes still presented identical silent features regarding size and intensity of hypofluorescence (Fig. 8A). However, depth analysis demonstrated the presence of highly prominent fluorescence (Fig. 8B). Active leakage had led to an elevated ICG level, with progressive filling of the RPE bleb (Fig. 8C).

Retinal Vascular Disease

Vascular leakage was visualized easily by FA, whereas the precise distribution of the extravasate often remained unclear. Exudation due to BRVO of the upper arcade covered the superior and central macular area in conventional FA (Fig. 9A). Extravasation of fluid into the retina with consecutive thickening resulted in detection of fluorescence in superficial layers normally appearing dark in depth analysis (Fig. 9B). Topographic imaging demonstrated the extent of retinal edema with respect to area and level of thickening (Fig. 9C). Focal laser coagulation was applied to reduce the amount of intraretinal fluid. Decreased extravasation was seen by conventional FA without any objective quantification (Fig. 10A). A reduction in superficial fluorescence was supported by topographic analysis (Fig. 10B). However, areas cleared from edema in contrast with persistent foci of active leakage was clearly differentiated by 3-D topography only (Fig. 10C).

DISCUSSION

Pathologic changes in retinochoroidal vascular functions such as impaired perfusion, proliferation, and exudation are not

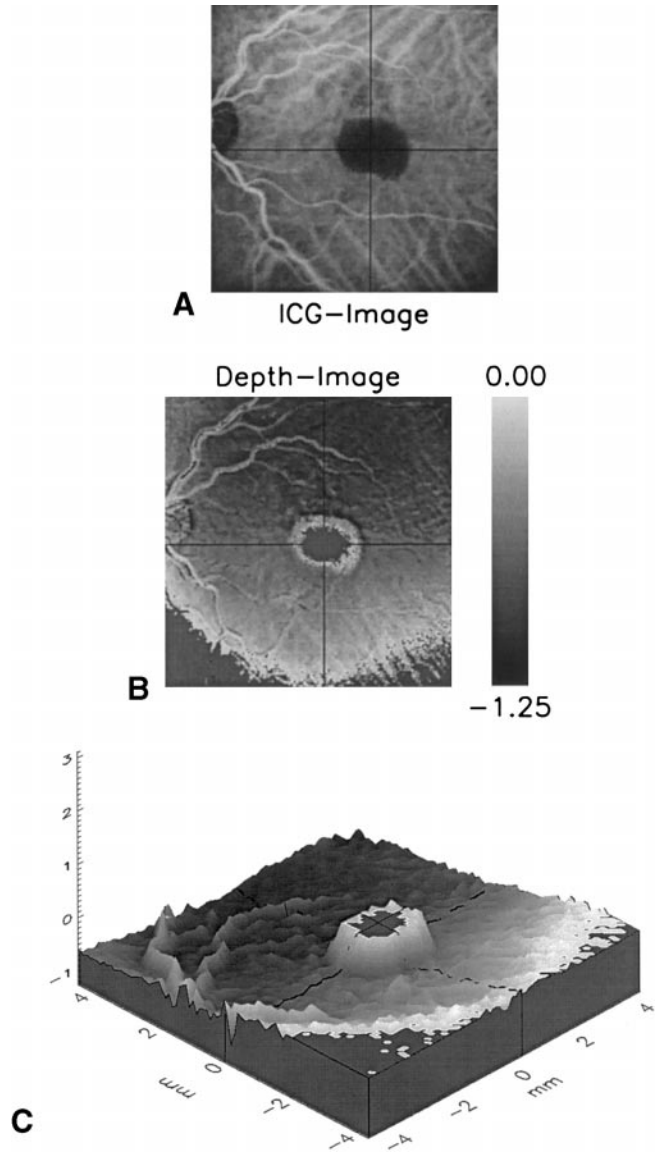

FIGURE 8. (**A**) In late-phase ICGA hypofluorescence is identical in shape and intensity compared with Figure 7A. (**B**) Topography of late-phase images reflects an elevated fluorescent border. (**C**) The level of dye filling of the PED is markedly elevated in late 3-D ICGA. Reduced signals from the center of the PED were detected, but were below the defined threshold for reliability.

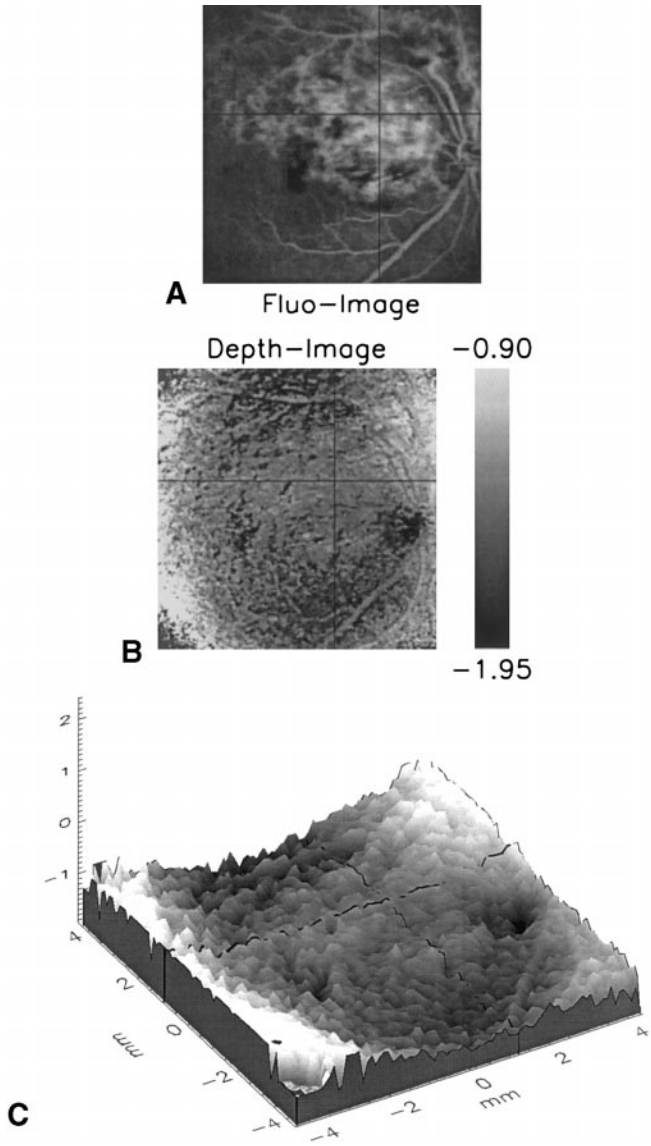

FIGURE 9. (**A**) Pretreatment FA in superior branch vein occlusion demonstrates diffuse leakage. (**B**) In topographic analysis, a bright area indicates prominent fluorescence due to intraretinal edema. (**C**) Swelling of the central retina by intraretinal fluid is seen in 3D-fluorescein topography.

identified sufficiently using conventional angiographic techniques. Low-contrast, vascular features obscured by leakage, masking by absorbing pigments, intensive background fluorescence, limited resolution, and insufficient depth separation strongly reduce the diagnostic value of routine imaging.

Topographic angiography is a newly developed modality able to extract 3-D data from tomographic confocal scanning angiograms using a digital image-processing technique. The actual topic distribution of fluorescent markers is detected at each time interval within intra- and extravascular compartments. Consequently, the 3-D morphology of the vascular architecture may be reconstructed in a noninvasive, in vivo mode and dynamic processes such as perfusion and extravasation may be evaluated qualitatively and quantitatively.

Under physiologic conditions, topographic angiography delineates the surface of the choriocapillary layer with the prominence of the overlying retinal vessels and the depression of the avascular optic nerve head.[12,13] To identify fundus findings that are detected only by topography and not by conventional angiography, well-defined clinical entities have to be analyzed by the method in significant numbers of patients, which is currently being done.

Because the information of fluorescence depth is analyzed independent of the absolute intensity, even small amounts of dye may be detected as long as they appear axially dislocated. Therefore, blocked fluorescence precluding identification of underlying diseases by conventional angiography are not of major importance in topographic imaging. CNV is detected underneath a hemorrhage, the borders of occult CNV are well defined, despite turbid extravasate and sub-RPE location. Otherwise unrevealing hypofluorescent lesions (e.g., PED or chorioretinal infiltrates) exhibit a specific pathophysiologic condition with clear identification of ICG in a presumably dye-free situation in conventional imaging. The nature of hypofluorescence becomes obvious: Perfusion defects actively filling with exudate are currently unknown in inflammatory chorioretinal

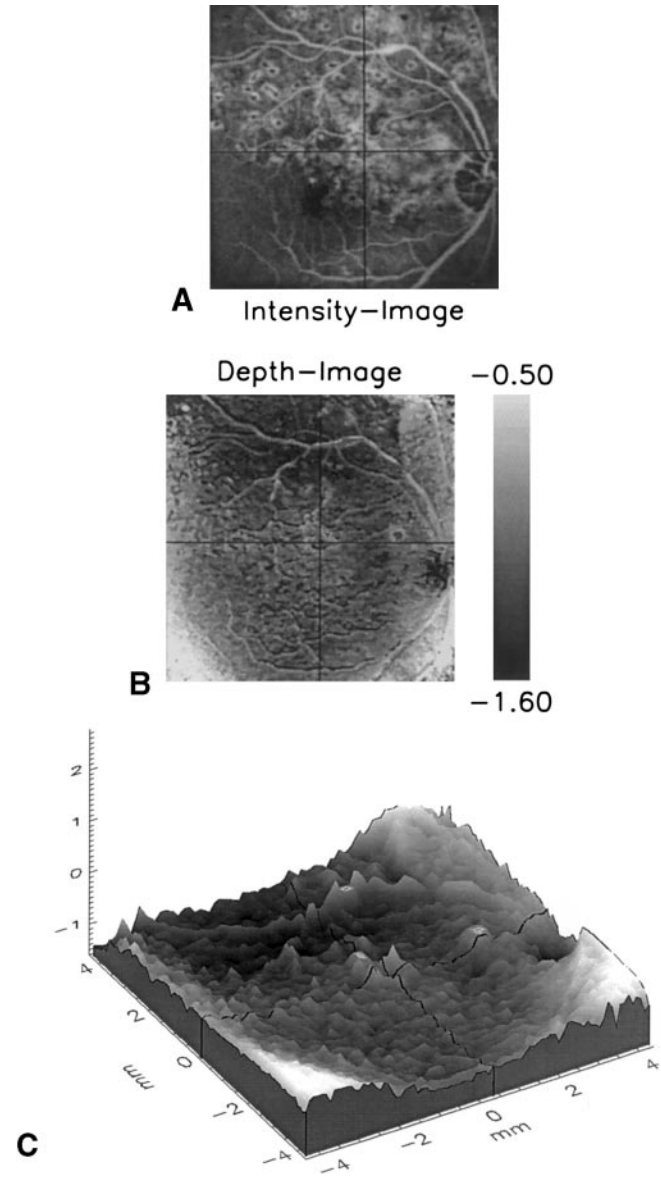

FIGURE 10. (**A**) Conventional FA 3 months after laser treatment demonstrates inhomogeneous persistent leakage. (**B**) The physiologic appearance of the posterior pole by topographic imaging is almost restored. (**C**) The surface of the central retina appears almost regular after resolution of fluid, with residual islands of edema centrally.

infiltrates, previously described as dark spots in conventional ICGA.[14] ICG pooling and progressive filling was shown conclusively by topographic angiography, despite the current hypothesis of ICG dye's absence in PED.[15] The efficient detection of even minimal dye concentrations also allows documentation of intraretinal fluid, as noted in retinal vascular disease with distinct delineation of the edematous zone using low-molecular-weight fluorescein as a marker. Clinically, FA is the routine procedure to document retinal extravasation, which appears to correlate directly with visual acuity and is therefore used for treatment indications.[16,17] The significant interobserver variation highlights the difficulties in objective leakage evaluation based on conventional FA,[17] a dilemma that might be resolved by topographic FA.

In respect to diseases with deeper or masked fluorescence, ICGA offers advantages over FA already in the conventional mode. Topographic analysis three-dimensionally differentiates the primarily low fluorescence emission of ICG very clearly so that ICG is detectable in pseudohypofluorescent lesions (e.g., occult CNV, hemorrhagic CNV, infiltrates, and PED). Although the SLO technique per se was shown to be superior to the high-resolution fundus camera,[18] conventional ICGA was successful in detecting vascular components of occult CNV in only 28% of eyes.[19] Well-defined borders of identified occult CNV were visible in 40% of eyes examined by conventional ICGA.[5] Digital contrast enhancement of 2-D ICGA alone increased the detection rate of well-defined boundaries from 36% to 58%.[20] Detection of occult CNV components, the major lesion type in neovascular ARMD, was successful in all topographic examinations of this series and should in general be significantly facilitated by the additional depth detection achieved by topographic ICG imaging.

Conventional ICGA to date has failed to provide objective definitions for fluorescence phenomena descriptively termed as hot spots and plaques due to insufficient structural recognition of lesion types. Plaques as a presumed correlate of CNV were observed and measured in size without identification of the underlying pathologic entity.[5,7,10,21] Occult CNV featured as ill-defined plaque by conventional ICGA was clearly identified as prominent vascular proliferation with well-defined borders and progression by topographic ICGA.[13] Two-dimensional reconstruction maps of histologic sections were used to morphologically correlate vascular channels in CNV with angiographic findings,[22,23] whereas topographic FA-ICGA per se routinely offers an in vivo morphometry of the vascular patterns in each patient.

Infrared imaging alone without the use of fluorescent probes provides topographic information of evolving sub-RPE CNV with an increased detection rate—however, without identification of the neovascular portion.[24–26] Fluorescence optical section (FOS) imaging obtained by scanning in a series of 40 cross-sectional images laterally separated by 50 μm achieves higher contrast and visualization of the retinal and subretinal vasculature.[27] This promising technique requires an additional instrumental set-up, images a small area only, and offers less depth resolution. Other 3-D imaging techniques include the retinal thickness analyzer (RTA), which does not differentiate between vascular and nonvascular structures,[28] and optical coherence tomography (OCT). This modality produces high depth resolution in cross-sectional tomographs, optimally on the order of 10 μm.[29] OCT is useful in the evaluation of sub- and intraretinal fluid as sequelae of CNV. The primary CNV pathology, however, appears as a localized thickening and fragmentation of the highly reflective RPE–choriocapillaris layer, rather than a well-defined vascular structure in the classic CNV subtype and was not identified at all if situated underneath the RPE.[30] As a second disadvantage OCT provides only static imaging and no documentation of fluid dynamics.[30,31]

Confocal topographic angiography offers a new qualitative imaging modality with high resolution, high contrast, and 3-D morphometry. Currently, a lateral and axial reproducibility of approximately 50 μm is achieved.[12] Resolution may be further improved by modification of the image alignment that would also smooth the slightly irregular surface seen in some of the relief pictures. A reduction of the image acquisition time and an efficient eye-tracking system could be advantageous. Averaging each data point with the neighboring pixels to a mean value of 9 pixels currently reduces resolution. Adaptation of a gaussian function to the axial intensity scan should further improve homogenous imaging. Further research is under way to improve this newly developed technology in respect to the alignment, threshold criteria, and increased resolution. The ability to quantify lesion dimensions and capture dynamic processes, such as extravasation and nonvascular barrier disturbances, with volumetric measurements introduces topographic angiography as a powerful tool to document the efficacy of current and innovative therapeutic strategies, such as photodynamic therapy and antiangiogenesis. From a diagnostic standpoint, the method offers revealing insights into the pathophysiology of chorioretinal vascular disease.

References

1. Nussenblatt RB, Kaufman SC, Palestine AG, et al. Macular thickening and visual acuity: measurements in patients with cystoid macular edema. *Ophthalmology*. 1987;94:1134–1139.
2. Early Treatment Diabetic Retinopathy Study Research Group. ETDRS report number 7: Early Treatment Diabetic Retinopathy Study design and baseline patient characteristics. *Ophthalmology*. 1991;98:741–756.
3. Bressler NM, Bressler SB, Gragoudas ES. Clinical characteristics of choroidal neovascular membranes. *Arch Ophthalmol.* 1987;105: 209–213.
4. Saito T, Komatsu Y, Mori S. A study of serum protein fraction binding to indocyanine green (ICG) by a combined method of immuno-electrophoresis and ICG fundus videosystem [in Japanese]. *Nippon Ganka Gakkai Zasshi*. 1996;100:617–623.
5. Regillo CD, Benson WE, Maguire JI, Annesley WH. Indocyanine green angiography and occult choroidal neovascularization. *Ophthalmology*. 1994;101:280–288.
6. Yannuzzi LA, Hope-Ross M, Slakter JS, et al. Analysis of vascularized pigment epithelial detachments using indocyanine green videoangiography. *Retina*. 1994;14:99–113.
7. Guyer DR, Yannuzzi LA, Slakter JS, Sorenson JA, Hope-Ross M, Orlock DA. Digital indocyanine green videoangiography of occult choroidal neovascularization. *Ophthalmology*. 1994;101:1727–1737.
8. Mainster MA, Timberlake GT, Webb RH, Hughes GW. Scanning laser ophthalmoscopy: clinical applications. *Ophthalmology*. 1982;89:852–875.
9. Webb RH, Hughes GW, Delori FC. Confocal scanning laser ophthalmoscope. *Appl Opt*. 1987;26:1492–1499.
10. Bartsch D-U, Weinreb RN, Zinser G, Freeman WR. Confocal scanning infrared laser ophthalmoscopy for indocyanine green angiography. *Am J Ophthalmol*. 1995;120:642–651.
11. Fitzke FW, Masters BR. Three-dimensional visualization of confocal sections of in vivo human fundus and optic nerve. *Curr Eye Res.* 1993;12:1015–1018.
12. Birngruber R, Schmidt-Erfurth U, Teschner S, Noack J. Confocal laser scanning fluorescence topography: a new method for three-dimensional functional imaging of vascular structures. *Graefes Arch Clin Exp Ophthalmol*. 2000;238:559–565.
13. Schmidt-Erfurth U, Noack J, Teschner S, Birngruber R. Confocal indocyanine green angiography with three-dimensional topography: results in choroidal neovascularization. *Ophthalmologe*. 1999;96:797–804.

14. Auer C, Bernasconi O, Herbort CP. Indocyanine green angiography features in toxoplasmic retinochoroiditis. *Retina*. 1999;19:22–29.
15. Flower RW, Csaky KG, Murphy RP. Disparity between fundus camera and scanning laser ophthalmoscope indocyanine green imaging of retinal pigment epithelium detachments. *Retina*. 1998; 18:260–268.
16. Arend O, Remky A, Elsner A, Bertram B, Reim M, Wolf S. Quantification of cystoid changes in diabetic maculopathy. *Invest Ophthalmol Vis Sci.* 1995;36:608–613.
17. Kylstra JA, Brown JC, Jaffe GJ, et al. The importance of fluorescein angiography in planning laser treatment of diabetic macular edema. *Ophthalmology*. 1999;106:2068–2073.
18. Scheider A, Kaboth A, Neuhauser L. The detection of subretinal neovascular membranes with indocyanine green and an infrared scanning laser ophthalmoscope. *Am J Ophthalmol.* 1992;113:45–51.
19. Gelisken F, Inhoffen W, Schneider U, Stroman G, Kreissig I. Indocyanine green videoangiography of occult choroidal neovascularization: a comparison of scanning laser ophthalmoscope with high-resolution digital fundus camera. *Retina.* 1998;18:37–43.
20. Maberley D, Cruess A. Indocyanine green angiography: an evaluation of image enhancement for the identification of occult choroidal neovascular membranes. *Retina.* 1999;19:37–44.
21. Pece A, Bolognesi G, Introini U, Pacelli G, Calori G, Brancato R. Indocyanine green angiography of well-defined plaque choroidal neovascularization in age-related macular degeneration. *Arch Ophthalmol.* 2000;118:630–634.
22. Chang TS, Freund KB, de la Cruz Z, Yannuzzi L, Green R. Clinicopathologic correlation of choroidal neovascularization demonstrated by indocyanine green angiography in a patient with retention of good vision for almost four years. *Retina.* 1994;14:114–124.
23. Grossniklaus HE, Cingle KA, Yoon YD, Ketkar N, L'Hernault N, Brown S. Correlation of histologic 2-dimensional reconstruction and confocal scanning laser microscopic imaging of choroidal neovascularization in eyes with age-related maculopathy. *Arch Ophthalmol.* 2000;118:625–629.
24. Hartnett E, Elsner A. Characteristics of exudative age-related macular degeneration determined in vivo with confocal and indirect infrared imaging. *Ophthalmology*. 1996;103:58–71.
25. Elsner AE, Burns SA, Weiter JJ, Delori FC. Infrared imaging of sub-retinal structures in the human ocular fundus. *Vision Res.* 1996;36:191–205.
26. Elsner AE, Staurenghi, Weiter J, Buzney S, Wolf S, Wald KJ. Infrared imaging in age-related macular degeneration: retinal pigment epithelium detachments. In: *Noninvasive Assessment of the Visual System*. *Ophthalmic and Visual Optics*. Monterey, CA: American Academy of Optometry; 1993;3:282–285.
27. Shahidi M, Zeimer R, Mori M, Blair N. A new method for noninvasive optical sectioning of the chorioretinal vasculature. *Invest Ophthalmol Vis Sci.* 1998;39:2733–2743.
28. Asrani S, Zou S, d'Anna S, Vitale S, Zeimer R. Noninvasive mapping of the normal retinal thickness at the posterior pole. *Ophthalmology*. 1999;106:269–273.
29. Puliafito CA, Hee MR, Lin CP, et al. Imaging of macular diseases with optical coherence tomography. *Ophthalmology*. 1995;102: 217–229.
30. Hee MR, Baumal CR, Puliafito CA, et al. Optical coherence tomography of age-related macular degeneration and choroidal neovascularization. *Ophthalmology*. 1996;103:1260–1270.
31. Antcliff RJ, Stanford MR, Chauhan DS, et al. Comparison between optical coherence tomography and fundus fluorescein angiography for the detection of cystoid macular edema in patients with uveitis. *Ophthalmology*. 2000;107:593–599.